JOURNAL OF AIRCRAFT
Vol. 48, No. 2, March–April 2011

Engineering Notes

Multigrid Acceleration and Chimera Technique for Viscous Flow Past a Hovering Rotor

Aiming Yang* and Xiaoquan Yang†
Fudan University,
200433 Shanghai, People's Republic of China

DOI: 10.2514/1.C031069

I. Introduction

ACCURATE simulation of the viscous flow around a helicopter rotor is still a challenging problem. To predict the blade loading accurately, the numerical method must have a capability to capture the vortical wake generated from the rotor blade tip precisely, which significantly affects the aerodynamic performance of the rotor. Therefore, both the numerical scheme with low numerical dissipation and sufficient dense mesh far away from the blade surface are required for rotor computations to simulate the tip vortex with minimal distortion. Furthermore, for a hovering case, a large numerical integration time is needed for the capture of the fully developed vortical wake [1]. In addition, the existence of incompressible flow near the root will also make the convergence slow. Compared with fixed-wing computations, hovering rotor computations not only require more accurate numerical scheme but also will take much more run time to converge.

During the past two decades many numerical methods [2–7] have been developed to simulate the viscous flow around a hovering rotor. The methods [2,3] with the single-block structured grid suffer from the grid-quality problem, because the mesh must be stretched and skewed to cover the complete computational domain and to match the periodic boundary condition. To avoid this problem, the chimera technique [4–7] suggested by Benek et al. [8] was introduced into hovering rotor computations. To capture the tip vortex without unphysical distortion and predict the blade loading accurately, some high-order schemes and vortex-adapted chimera methods [6,7] were presented. Although significant advances in the accurate simulation of the tip vortex have been made with these advanced methods, the large computation cost and the low robustness, as well as the complexity make them far away from engineering applications.

As mentioned above, hovering rotor computations, especially the computations with high-order methods, require more run time to converge than their fixed-wing counterparts. A few attempts [1,9,10] have been made to use multigrid methods to accelerate the convergence of hovering rotor calculations. Up to now, there is few works concerning the multigrid method for the viscous flow computation about a hovering rotor based on overset grids.

The main objective of the present study is to develop an efficient multigrid algorithm coupled with chimera grids for Navier–Stokes computations about a hovering rotor. It should be mentioned that the experience of this work can be extended to accelerate the computation about a rotor in forward flight using moving overset grids, which is the main motivation of this research. Furthermore, this experience can also be the basis of the future multigrid computation using high-order methods and chimera grids for rotor flows.

II. Governing Equations and Numerical Methods

The governing equations for the flowfield are the thin layer Reynolds-averaged Navier–Stokes equations written in a reference frame rotating with a constant angular velocity $\boldsymbol{\omega}$

$$\frac{\partial}{\partial t}\int_V \mathbf{W}\,\mathrm{d}V + \oint_{\partial V}\mathbf{H}\cdot\mathbf{n}\,\mathrm{d}S - \oint_{\partial V}\mathbf{H}_v\cdot\mathbf{n}\,\mathrm{d}S + \int_V \mathbf{G}\,\mathrm{d}V = 0$$
$$\mathbf{G} = [0 \quad \rho(\boldsymbol{\omega}\times\mathbf{q})_x \quad \rho(\boldsymbol{\omega}\times\mathbf{q})_y \quad \rho(\boldsymbol{\omega}\times\mathbf{q})_z \quad 0]^{\mathbf{T}} \tag{1}$$

where ρ, $\mathbf{q}$, W, H, and H_v are fluid density, fluid velocity, conserved quantity, inviscid flux, and viscous flux, respectively. The Baldwin–Lomax turbulence model [11] is used to close the RANS equations.

The cell-centered finite volume method with the Roe's flux-difference splitting scheme [12] is employed. The MUSCL [13] scheme with the van Leer limiter is used to get high-order accuracy. The implicit lower–upper symmetric-Gauss–Seidel method scheme [14] is used as the time integration method.

III. Multigrid Method for Chimera Grids

The general introduction of the multigrid method can be found in [1]. This section will focus on the determination of the hole cells and fringe cells on the coarse grid, which is the most important work in this algorithm.

Assuming a coarse cell contains one or more fine-grid hole cells, then the coarse cell is labeled as a coarse grid hole cell. Before specifying the fringe cells and the computational cells on the coarse grid, we should shift attention to these definitions on the fine-grid. For convenience, a two-dimensional mesh is demonstrated in Fig. 1. A hole cell is tagged as a solid square, a fringe cell is tagged as a hollow circle, and a computational cell is tagged as a solid circle, respectively. Cell E is a coarse grid cell consisting of four fine-grid cells, i.e., cell A, cell B, cell C and cell D. According to the above definition, this coarse grid cell is a hole cell because the cell A is a fine-grid hole cell. If only the neighbor cells along the mesh lines are labeled as fringe cells, then we can find in Fig. 1a that the coarse grid cell E consists of both the fine-grid hole cell (cell A) and the fine-grid computational cell (cell C). This will lead to the fine-grid computational cell (cell C) without prolongated correction from the coarse grid, when performing prolongation from the coarse grid to the fine grid, because the cell E is a coarse grid hole cell. To avoid this situation, the neighbor cells at the corners are also specified as fine-grid fringe cells, which is depicted in Fig. 1b.

Considering the need for sufficient overlap area, only one layer of coarse grid fringe boundary is required. It should be emphasized that the coarse grid fringe cells cannot be specified directly as the neighbor cells of the coarse grid hole cells. This improper definition will lead to the problem that a coarse grid cell containing one or more fine-grid fringe cells is not categorized as a coarse grid fringe cell, but a coarse grid computational cell. As a consequence, the forcing function for this coarse grid cell cannot be evaluated reasonably because no value is assigned to the residuals of fine-grid hole cells. Therefore, a coarse grid fringe cell should be specified as the cell which is a nonhole cell containing one or more fine-grid fringe cells.

Received 18 April 2010; revision received 24 November 2010; accepted for publication 26 November 2010.

*Associate Professor, Department of Mechanics and Engineering Science; amyang@fudan.edu.cn.

†Doctoral Candidate, Department of Mechanics and Engineering Science.

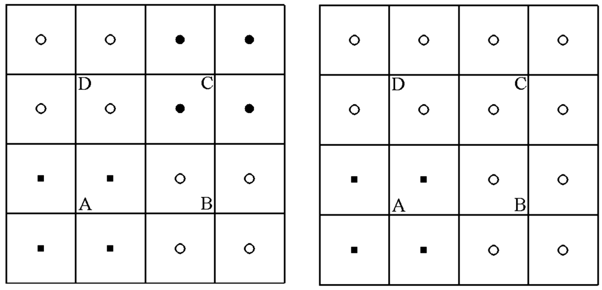

a) b)

Fig. 1 The two definitions of the fine-grid fringe cells.

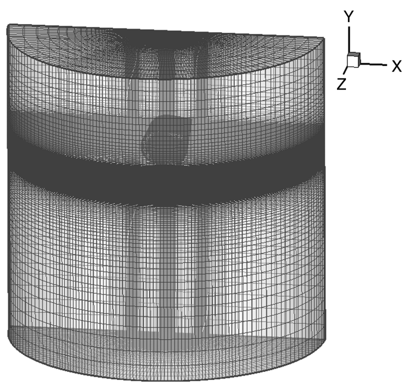

Fig. 2 Chimera grids for a hovering rotor.

IV. Results

Two cases with the tip Mach number 0.877 (case 1) and 0.61 (case 2) for the two-bladed Caradonna–Tung rotor are computed and compared with experimental results [15].

The chimera grids for this rotor are shown in Fig. 2. This grid system consists of a body-conforming *C-H* mesh ($160 \times 96 \times 68$) around the blade and a cylindrical *H-H* mesh ($104 \times 92 \times 180$) as the background grid. This mesh extends about 3 radii in radial direction, about 3 radii above the blade surface and about 6 radii below the blade surface, respectively. The hole boundary of the background grid is about one chord away from the blade surface in the normal direction and about half of one chord away from the blade tip in the spanwise direction.

The convergence criteria is defined as 4 orders of magnitude reduction in density residual, meanwhile the oscillation amplitude of the total thrust coefficient is less than 0.5% of its final value. To provide a uniform measure of computational effort, a work unit is defined as being equivalent to the computational effort for one iteration on the fine grid. For instance, for three-dimensional cases, eight iterations on the coarse grid are equivalent to one iteration on the fine grid. In this study, only a two-level multigrid is used.

The comparison between the single grid and multigrid computations is shown in Table 1. Among all the combinations with different number of iterations at every mesh level, the speed-up ratio with two iterations on the fine mesh and eight iterations on the coarse mesh is the highest. Therefore, only the multigrid method with this combination is compared with the single grid method. From this table, the speed-up ratio in terms of work unit is about 5.77 for case 1 and 6.69 for case 2. Since the additional work for the implementation of the multigrid method occupy the run time, the speed-up ratio in terms of CPU time, which is also shown in this table, is about 5.0 for case 1 and 5.86 for case 2.

Table 1 Convergence rate and the total thrust coefficients

	Single grid (Case 1)	2V-2-8 (Case 1)	Single grid (Case 2)	2V-2-8 (Case 2)
Work units	7770	1347	8002	1197
Work hours	51.80	10.23	53.35	9.10
Convergence rate	——	5.06	——	5.86
Thrust coefficient (numerical result)	0.00495		0.00831	
Thrust coefficient (experimental data)	0.00464		0.00807	
Error	6.68%		2.97%	

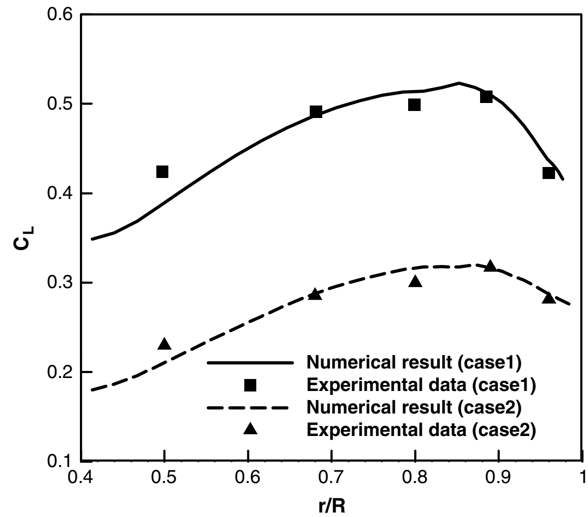

Fig. 3 Spanwise sectional thrust coefficient distributions.

The sectional thrust coefficient distributions are presented in Fig. 3. For both cases, the overall agreement between the computed and measured data is good. For the radial positions at about 50% span and 80% span, some larger differences are observed. Table 1 also presents the total thrust coefficients. A slight overprediction is demonstrated for both cases, which is about 6.68% for case 1 and 2.97% for case 2. All these differences in thrust coefficients are mainly due to the imprecise representation of the tip vortex.

V. Conclusions

An upwind Navier–Stokes solver based on chimera grids has been developed to simulate the viscous flow past a helicopter rotor in hover. To accelerate the computation, an efficient multigrid algorithm for chimera grids is presented.

For both transonic case and subsonic case, the speed-up ratio with two-level multiple grids is greater than 5.0. This significant acceleration effect also implies the correctness of the treatments presented in this research. This experience is also very useful for the implementation of multigrid acceleration coupled with moving overset grids for the simulation about a rotor in forward flight.

Although there are some larger differences for sectional thrust coefficients at some radial stations, the overall agreement is good for both cases. A slight overprediction of the total thrust coefficient is observed for both cases. All these differences can be explained by the imprecise representation of the tip vortex. The numerical diffusion inherent in the present numerical scheme and no mesh adaption for the vortex are responsible for this vortex distortion. Solving these problems are our research directions in the future.

Acknowledgment

This work reported here has been funded by the Shanghai Municipal Natural Science Foundation under contract no. 09ZR1411400.

References

[1] Allen, C. B., “Multigrid Acceleration of an Upwind Euler Method for Hovering Rotor Flows,” *The Aeronautical Journal*, Vol. 105, No. 1051, 2001, pp. 517–524.

[2] Srinivasan, G. R., Baeder, J. D., Obayashi, S., and McCroskey, W. G.,

"Flowfield of a Lifting Rotor in Hover: A Navier-Stokes Simulation," *AIAA Journal*, Vol. 30, No. 10, 1992, pp. 2371–2378. doi:10.2514/3.11236

[3] Wake, B. E., and Baeder, J. D., "Evaluation of a Navier–Stokes Analysis Method for Hovering Performance Prediction," *Journal of the American Helicopter Society*, Vol. 41, No. 1, 1996, pp. 7–17. doi:10.4050/JAHS.41.7

[4] Pomin, H., and Wagner, S., "Navier–Stokes Analysis of Helicopter Rotor Aerodynamics in Hover and Forward Flight," *Journal of Aircraft*, Vol. 39, No. 5, 2002, pp. 813–821. doi:10.2514/2.3001

[5] Strawn, R. C., and Djomehri, M. J., "Computational Modelling of Hovering Rotor and Wake Aerodynamics," *Journal of Aircraft*, Vol. 39, No. 5, 2002, pp. 786–793. doi:10.2514/2.3024

[6] Hariharan, N. S., and Sankar, L. N., "First-Principles Based High-Order Methodologies for Rotorcraft Flowfield Studies," *Proceedings of 55th Annual Forum of the American Helicopter Society*, American Helicopter Society, Alexandria, VA, 1999, pp. 1921–1933.

[7] Duraisamy, K., and Baeder, J., "High Resolution Wake Capturing Methodology for Hovering Rotors," *Journal of the American Helicopter Society*, Vol. 52, No. 2, 2007, pp. 110–122. doi:10.4050/JAHS.52.110

[8] Benek, J. A., Buning, P. G., and Steger, J. L., "A 3-D Chimera Grid Embedding Technique," AIAA Paper 85-1523, 1985.

[9] Allen, C. B., "Multigrid Convergence of Inviscid Fixed and Rotary-wing Flows," *International Journal for Numerical Methods in Fluids*, Vol. 39, No. 2, 2002, pp. 121–140. doi:10.1002/fld.282

[10] Allen, C. B., "Convergence of Steady and Unsteady Formulations for Inviscid Hovering Rotor Solutions," *International Journal for Numerical Methods in Fluids*, Vol. 41, No. 9, 2003, pp. 931–949. doi:10.1002/fld.474

[11] Baldwin, B., and Lomax, H., "Thin Layer Approximation and Algebraic Model for Separated Turbulent Flow," AIAA Paper 78-0257, 1978.

[12] Roe, P. L., "Approximate Riemann Solvers, Parameter Vectors and Difference Schemes," *Journal of Computational Physics*, Vol. 43, No. 2, 1981, pp. 357–372. doi:10.1016/0021-9991(81)90128-5

[13] Anderson, W. K., Thomas, J. L., and van Leer, B., "Comparison of Finite Volume Flux Vector Splittings for the Euler Equations," *AIAA Journal*, Vol. 24, No. 9, 1986, pp. 1453–1460. doi:10.2514/3.9465

[14] Yoon, S., and Jameson, A., "Lower-Upper Symmetric-Gauss-Seidel Method for the Euler and Navier–Stokes Equations," AIAA Paper 87-0600, 1987.

[15] Caradonna, F. X., and Tung, C., "Experimental and Analytical Studies of a Helicopter Rotor in Hover," NASA TM-81232, 1981.